The mechanism of CO and CO2 hydrogenation to methanol over Cu based catalysts**

Felix Studt,*‡[a,b] Malte Behrens,*‡[c,d] Edward L. Kunkes,[c] Nygil Thomas,[c] Stefan Zander,[c] Andrey Tarasov,[c] Julia Schumann,[c] Elias Frei,[c] Joel B. Varley,[b,e] Frank Abild-Pedersen,[a,b] Jens K. Nørskov,[a,b] Robert Schlögl[c,f]

[a]   Dr. F. Studt, Dr. F. Abild-Pedersen, Prof. J. K. Nørskov

SUNCAT Center for Interface Science and Catalysis

SLAC National Accelerator Laboratory

2575 Sand Hill Road, Menlo Park, CA 94025, USA

E-mail: studt@slac.stanford.edu

[b]   Dr. F. Studt, Dr. J. B. Varley, Dr. F. Abild-Pedersen, Prof. J. K. Nørskov

Department of Chemical Engineering, Stanford University

Stanford, CA 94305, USA

[c]   Prof. M. Behrens, Dr. E. L. Kunkes, Dr. N. Thomas, Dr. S. Zander, Dr. A. Tarasov, J. Schumann, Dr. E. Frei, Prof. R. Schlögl

Department of Inorganic Chemistry

Fritz-Haber-Institut der Max-Planck-Gesellschaft

Faradayweg 4-6, 14195 Berlin, Germany

[d]   Prof. M. Behrens

Faculty of Chemistry and CENIDE, Universität Duisburg-Essen

Universitätsstr. 5-7, 45141 Essen, Germany

E-mail: malte.behrens@uni-due.de

[e]   Dr. J. B. Varley

Lawrence Livermore National Laboratory

Livermore, CA 94550, USA

[f]   Prof. R. Schlögl

Heterogeneous Reactions Department

Max-Planck-Institut for Chemical Energy Conversion

Stiftstr. 34-36, 45470 Mühlheim an der Ruhr, Germany

‡   These authors contributed equally to this work.

**   Supporting information for this article is given via a link at the end of the document.

Abstract: Methanol, an important chemical, fuel additive and precursor for clean fuels, is produced by hydrogenation of carbon oxides over Cu-based catalysts. Despite the technological maturity of this process, the understanding of this apparently simple reaction is still incomplete with regard to the reaction mechanism and the active sites. Regarding the latter, recent progress has shown that stepped and ZnOx-decorated Cu surfaces are crucial for the performance of industrial catalysts. Herein, we integrate this insight with additional experiments into a full microkinetic description of methanol synthesis. In particular, we show how the presence or absence of the Zn promoter dramatically changes not only the activity, but unexpectedly the reaction mechanism itself. The Janus-faced character of Cu with two different sites for methanol synthesis, Zn-promoted and unpromoted, resolves the long-standing controversy regarding the Cu-Zn synergy and adds methanol synthesis to the few major industrial catalytic processes that are described on an atomic level.

Introduction

Industrial methanol synthesis is conducted at elevated pressure and temperature from a syngas mixture containing CO_2, CO and H_2. Typically, a $Cu/ZnO/Al_2O_3$ catalyst is employed at 50–100 bar and 200–300 °C.[1] As in many industrial catalytic processes, the technological application of methanol synthesis has preceded the full understanding of the underlying chemistry. Thus, the process has been operated for decades on empirical knowledge. The exact reaction mechanisms and the interplay of the catalyst's surface properties with the feed gases are debated to this day.[1-2] Among the most important open questions are the nature of the preferred carbon source for methanol – CO[3] or CO_2[4] - and the effect of the so-called "Cu-Zn synergy" considered as having either no unique role,[2a] i.e. mere structural promotion, or being essential for the active site.[2c][5] Part of these discussions arise due to the difficulty of obtaining data for the industrial $Cu/ZnO/Al_2O_3$ catalysts under realistic working conditions.[5] In addition, the variety of different copper based catalysts showing vastly contradicting behavior with respect to changes in the feed[6] complicates the selection of a suitable model system.

Herein, we integrate these different models and provide evidence for a consistent and comprehensive mechanistic picture of methanol synthesis by studying both above-mentioned questions on realistic high performance catalysts in a combined way using a joint approach of dedicated experiments with extensive theoretical modeling. We consider two limiting cases for Cu based catalysts with high surface area: copper nanoparticles supported on the irreducible MgO and Cu particles of comparable size and shape supported on ZnO. The presence of ZnO leads to a vividly debated synergetic effect of the components in this catalyst.[2b, 2c, 7] This effect was confirmed, for example, for a nano-structured Cu/MgO catalyst, which despite its relatively high Cu surface area was drastically inferior to a reference Cu/ZnO catalyst in methanol synthesis from CO_2-containing synthesis gas.[6b] Similarly high Cu surface areas of Cu/ZnO and ZnO-free systems have to this date only been achieved with MgO due to the analogous synthesis protocol as described previously,[6b] which ensures a general high comparability of the respective catalysts, wherein ZnO and MgO both equally fulfilled the role as a physical support for Cu. Thus, the catalytic behavior must be attributed to an additional non-structural promoting role of ZnO, which is in agreement with the observation that strong-metal-support interaction (SMSI) plays a key role in achieving a Zn-decorated surface state of Cu.[8] The SMSI is only present for reducible ZnO, where it affects the adhesion between Cu and ZnO,[2b, 9] but not for non-reducible MgO. As a result of SMSI, Zn atoms are supplied to the Cu surface, where they can get involved in the active site motif of the working catalyst.[2c, 5, 10]

Results and Discussion

Figure 1 shows the methanol synthesis activity of the Cu/MgO in different feed gases (all experimental details are reported as Supporting Information). As determined by H_2 chemisorption,[11] the Cu surface areas were 13.6 mCu_2/g for Cu/MgO and 14.7 mCu_2/g for Cu/ZnO/Al2O3. This similar high Cu dispersion allowed a direct comparison of these performance catalysts at the same conditions regarding temperature, pressure and catalyst mass without any re-scaling in Figure 1A rendering these catalysts a suitable materials basis to study the effect of presence and absence of ZnO on Cu-based methanol synthesis catalysts. Interestingly, both catalysts exhibit a dramatically different behavior in the presence or absence of CO_2 in the feed gas. While the Cu/MgO catalyst shows a high methanol formation rate in a CO/H_2 mixture (case A), its Cu/ZnO-based counterpart is highly active in $CO_2/CO/H_2$ (case D). A feed gas switching experiment (Figure 1a) shows that the performance of the Cu/ZnO deteriorates in CO/H_2 (case C), which is fully reversible upon re-addition of CO_2 into the feed excluding sintering or any other irreversible effect as the origin of this behavior. Conversely, the Cu/MgO catalyst rapidly loses its activity in a $CO_2/CO/H_2$ feed (case B), which is completely re-established in CO/H_2 at long time on stream. This result confirms that Cu is in general capable of converting CO as well as CO_2 to methanol at industrially relevant rates. In support of Nakamura's view,[2c] we propose that contradicting views on methanol synthesis can easily arise if CO and CO_2 hydrogenation are not considered separately. Industrial conditions are characterized by the presence of ZnO in the catalysts and of CO_2 in the feed and are only inadequately simulated by ZnO-free model catalysts (a family represented here by Cu/MgO).

The Cu catalysts reveal a Janus-faced behavior and work only efficiently in either the absence of CO_2 (Cu/MgO, case A) or in the presence of a CO_2/CO mix (Cu/ZnO, case D), respectively, but not vice versa. We determined the carbon source for methanol formation in the syngas mixture containing 57% CO_2 (as $CO_2/[CO+CO_2]$) by $^{13}CO_2$ labeling and found that the vast majority of the methanol formed (Figure 2) was from CO_2 in both cases. This finding was independent of whether we employed the Cu/ZnO/Al2O3 catalyst containing a high turnover rate (case D) or the Cu/MgO catalyst that exhibits a rather poor rate towards methanol (case B, for details see Supporting Information). Concerning the Cu/ZnO-based material, this result is in good agreement with earlier radio-isotope labeling studies[4, 12] and CO_2 pulse experiments[2h] reported in the literature. In a recent labeling experiment on Cu/SiO2, 78% of the formed methanol was found to stem from CO_2 at 513K and 6 bar.[2d] Our findings for the Cu/MgO catalyst are generally in agreement and indicate that CO_2 acts both as a poison (by efficiently suppressing CO conversion) and as a precursor for methanol formation, although the rate of CO_2 hydrogenation on Cu/MgO is rather low.
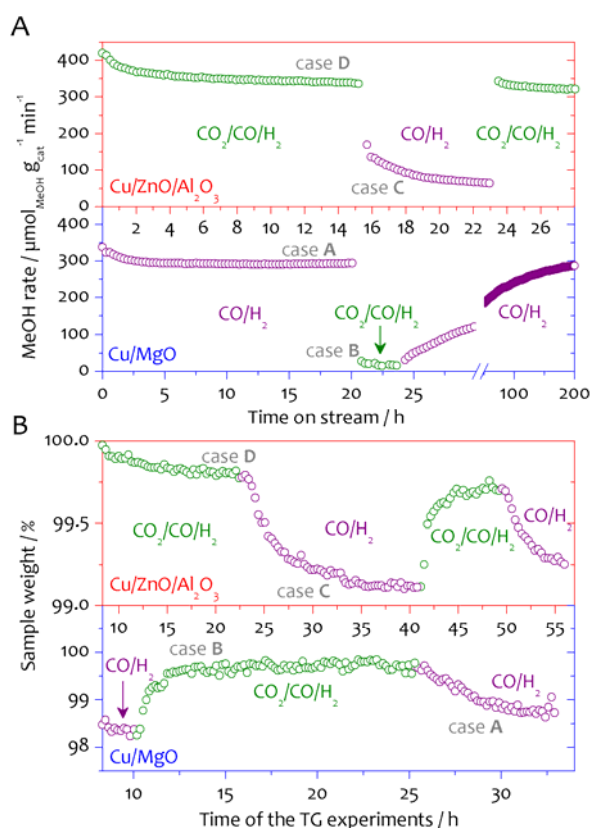
Figure 1. Methanol formation rates of Cu/ZnO/Al2O3 (upper panels) and Cu/MgO (lower panels) with time-on-stream (A) and in situ-thermogravimetry (B). Both experiments were conducted at 503 K and 30 bar in different feed gases. The gas switching is indicated by color changes (CO2/CO/H2/inert (8:6:59:27): dark green; CO/H2/inert (14:59:27): purple). A detailed description of both experiments and the catalyst is provided in the Supporting Information.

A gravimetric in situ-measurement under reaction conditions showed that both catalysts gain weight in CO2-containing feed and reversibly lose that weight when the feed is switched to CO only (Figure 1b). As brass or bulk carbonate formation can be excluded based on control experiments (see Supporting Information), we attribute the reversible weight change to the adsorbate coverage of the catalyst's surface under reaction conditions. Formate is well-known to be formed on Cu surfaces and has been observed to be the most abundant surface species during methanol synthesis in several studies.[13] Thus the observed weight changes suggest that in a CO2 containing syngas mix both, the Cu/MgO and Cu/ZnO catalyst are similarly covered with a formate-containing adsorbate layer, which is slowly released or replaced by lighter adsorbates as the CO2 feed is turned off. The presence of highly sticking carbon species on the catalyst's surface under working conditions is also supported by a sustained methanol production if the feed is switched from COx/H2 to H2/Ar (see Supporting Information).

Figure 2 shows the intrinsic, i.e. Cu surface area-normalized, methanol formation rates near differential conditions as a function of the CO2 concentration in the feed gas. In addition to the inverse behavior of Cu/MgO and Cu/ZnO (cases A-D), it can be seen that upon the first addition of CO2 the activity of Cu/ZnO/Al2O3 rises precipitously and further increases with an increase in CO2 content, strongly suggesting that CO2 is converted to methanol rather than CO. Note that only if the experiments are conducted at higher conversions away from the differential regime, a volcano-type behavior with CO2 concentration[2f, 3] can be observed, which is due to product inhibition by water as has been shown by Sahibzada et al.[14] The resulting maximum in methanol formation usually

observed at low CO2 concentrations is sometimes related to "CO2-promoted methanol synthesis" – a term that does not reflect that CO2 is the major carbon source for methanol.

In case of Cu/MgO, the situation is reversed and the high CO hydrogenation rate is suddenly quenched in the presence of even small amounts of CO2. The addition of 5 wt.% ZnO to the Cu/MgO catalyst by impregnation[6b] can revert its behavior. This result provides evidence that the ZnO promoter plays a decisive role for the catalytic properties of Cu in industrial catalysts as it was observed for model catalysts.[2c] The behavior of our catalysts in a CO2/H2 feed is similar to that in the CO/CO2/H2 mix and the intrinsic activities are in a similar range like TOF values determined in surface science experiments on model materials. The activity of Cu/MgO is found to be almost identical to the TOF found for Cu(111) by Fujitani et al.[15] and one third of that of polycrystalline Cu foil as determined by Campbell and co-workers.[16] The intrinsic activity of Cu/ZnO/Al2O3 in CO2 hydrogenation is, however, 16x higher than that of Cu/MgO and slightly above the TOF determined by the former authors for a Zn-doped Cu(111) single crystal.

The quenching effect of the Cu/MgO catalyst upon CO2 addition seen in Figure 2 is very drastic. This is on the one hand clearly due to its extraordinary high initial methanol synthesis activity in pure CO/H2 thanks to the synthesis method leading to high Cu dispersion, but might be additionally amplified by the surface basicity of MgO on the other hand. Indeed, it seems reasonable to assume that the poisoning effect of formate is stronger on very basic catalysts. However, also Cu supported on amphoteric Al2O3 or La2O3 showed a clear decrease in methanol synthesis activity upon addition of CO2 to CO/H2, but a much lower performance level not comparable to industrial performance catalysts (see SI, Fig. S2). Indeed, in case of Cu/Al2O3 the methanol synthesis activity exhibit a faster recovery with increasing CO2 level than in case of Cu/MgO indicating that poisoning was less severe on this less basic support. Thus, while the exact strength of the poisoning effect will likely depend on the type of irreducible non-ZnO support, we can assume that the general effect of CO2 poisoning in ZnO-free catalysts compared to the beneficial effect of CO2 on the methanol formation rate in Cu/ZnO is a general feature that is attributed to the presence or absence of ZnO as expressed most clearly by the comparison of Cu/MgO with two ZnO-containing performance catalysts in Figure 2.
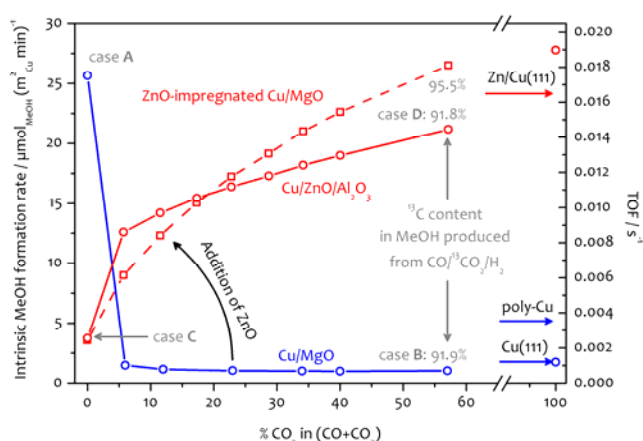

Figure 2. Intrinsic methanol formation rate of a Cu/ZnO/Al2O3 (red), the Cu/MgO (blue) and an Cu/MgO/ZnO catalyst (dashed) that was obtained by impregnation of ZnO onto Cu/MgO, as a function of the CO2 concentration in the feed gas ([CO2+CO]/H2/inert = 14:59:27) at 503 K and 30 bar. The data points correspond to the steady state activity after an equilibration time of 4 h for each measurement. The direction of concentration change was from low to high CO2 concentration for

Cu/MgO and in the opposite direction for the ZnO-containing catalysts for reasons discussed in the Supporting Information. The 13C data given on the right hand side of the plot correspond to independent isotope labeling experiments that have been carried out at the same conditions in the CO2-richest feed at steady state (13CO2:CO:H2:inert = 8:6:59:27). The axis on the right hand side shows corresponding TOFs from model studies, polycrystalline Cu (blue arrow "poly-Cu")[31] and Cu(111) single crystal before (blue arrow "Cu(111)") and after Zn deposition on Cu(111) (red arrow, coverage   Zn = 0.19)[30] for CO2/H2 feed. The Literature values have been corrected for pressure and temperature as described in the Supporting Information together with the experimental details. The measured rates in 100% CO2 (squares, blue: Cu/MgO; red: Cu/ZnO/Al2O3) were separately obtained with fresh samples as described in the Supporting Information.

In order to understand the different catalytic behavior of the Cu/MgO and Cu/ZnO as well as the role of CO and CO2 as feed for methanol synthesis we applied density functional theory (DFT) calculations on two stepped model surfaces, Cu(211) (representing Cu/MgO and hereafter called the Cu-site) and a fully Zn-covered Cu211 step (representing Cu/ZnO and hereafter called the Zn-site), see Figure 3, to model the two limiting cases. While the full elucidation of the true surface properties under working conditions remains challenging, we justify our structural model of the Zn-site based on the experimental and theoretical results presented previously,[5] where surface enrichment of Zn on the Cu particles was observed by XPS and HRTEM. Compared to our earlier work, a new generation of model for the Zn-site was employed in this study. It consists of the 211 Cu surface with a fully Zn-decorated step opposed only partial substation of Cu and Zn in the step. This is certainly an extreme case and there will be some Cu atoms present in the steps in realistic systems. This can also be seen in Figure 2 where the CO hydrogenation activity for Cu/ZnO catalysts is not entirely suppressed. The experimentally observed damping of this reaction by the presence of Zn atoms, however, can only be modelled using the new fully Zn-covered step model, as the formerly used model provides high CO hydrogenation activity by a too large number of coordinatively unsaturated Cu sites. We note that during the preparation of this paper, a microkinetic modelling of methanol synthesis using our old model was presented by van Rensburg et al.[2j] Recently, further experimental support for the surface alloying model has been provided by Kuld et al, who found metallic Zn on the surface of reduced realistic Cu/ZnO catalysts by Auger emission spectroscopy.[10b] We employed the BEEF-vdW functional[17] as it has been shown that only the inclusion of dispersion forces allows a quantitative description of methanol synthesis on copper catalysts.[18] The importance of surface steps in the structural motif has recently been verified experimentally and theoretically for the industrial catalyst[2j, 5] and is in agreement with the structure sensitivity of the methanol synthesis reaction, which was established by the group of Campbell, who using clean Cu found the highest specific activity for a Cu(110) surface,[13d] which in the present context can be viewed as a heavily stepped (111) surface. The reported TOF corrected for the different conditions used in Campbell's study amounts to 1.34×10^{-2} s^{-1}, markedly higher than Cu(111). For nano-sized systems, an additional promoting role of ZnO attributed to this morphological effect on pure Cu sites was proposed.[2b, 2e, 10a] The energetics calculated here on the two model surfaces are employed in a microkinetic model. This model uses the established pathways for CO and CO2 hydrogenation[19] calculating the methanol rate from CO and CO2 under differential conditions (see Supporting Information). Figure 3 shows the results of the DFT calculations and the microkinetic modeling for the two structural motifs as a function of CO2 concentration in the feed gas.

The free energy diagram of the hydrogenation of CO and CO2 shows that both reactions exhibit a maximum free energy barrier of about 1.5 eV on the Cu-site. The formation of formate is downhill in free energy indicating a substantial coverage of this species in agreement with the data of Figure 1B and with the results of van Rensburg et al.[2j] When Zn is introduced into the steps (Zn-site) all intermediates and transition-states that bind through an oxygen atom are stabilized. While

all carbon-bound intermediates can still bind on partially Zn substituted Cu steps[5] they become severely destabilized upon full substitution of Cu atoms with Zn. The Cu-site and the Zn-site can thus be seen as the two extreme cases for methanol synthesis catalysts. The addition of Zn hence acts as a promoter for the hydrogenation of CO2 since all its intermediates for this pathway bind to the surface through an oxygen atom. Since most intermediates of the CO hydrogenation pathway bind through the C atoms, a full layer of Zn will block the step sites for this process. The results of the microkinetic modeling confirm these conclusions and are shown in the lower panels for the case of the Cu-site (blue) as well as Zn-site (red). The Cu-site is quite active for CO hydrogenation, its activity decreases significantly, however, with CO2 concentration in the feed. This is because formate covers the surface and decreases the availability of free sites[2j] as shown in Figures 2 and 3. All calculated changes in surface coverage with feed gas composition are consistent with the gravimetric measurements (Figure 1b). Formate does not only act as a poison but it is an intermediate in the hydrogenation of CO2. CO2 hydrogenation on the Cu site is slow so that an overall decrease in total hydrogenation rate is observed (see also insert in Figure 3). Interestingly, our kinetic model predicts that despite the low CO2 hydrogenation rate, the carbon source gradually changes from CO to CO2 with increasing CO2 concentration in the feed due to the strong site blocking effect of formate on CO hydrogenation. Thus, the fraction of methanol formed from CO2 follows the formate coverage at the surface. This as well as the trend in total hydrogenation activity is in good qualitative agreement with the experiments described above and well within the accuracy of DFT.[20]
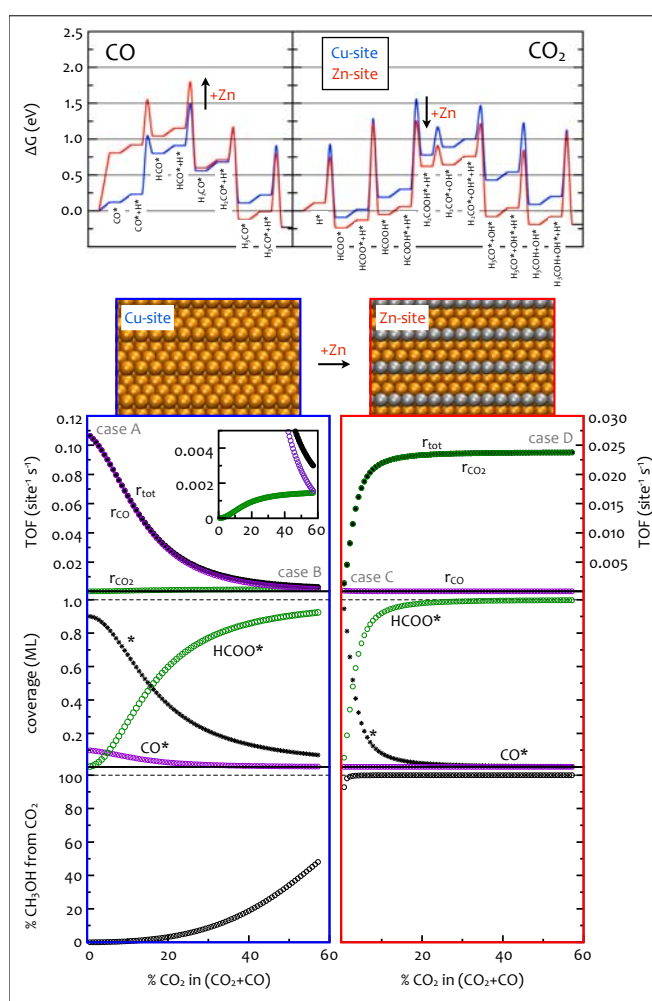
Figure 3. Top: Free energy diagram of CO (left) and CO2 (right) hydrogenation to methanol at 503 K on the Cu-site (blue line) and Zn-site (red line) as obtained from the DFT calculations. Bottom: Turnover frequencies, coverages, and carbon percentages from CO2 in methanol product for the Cu-site (left) and the Zn-site (right) as a function of CO2 concentration in the feed gas. Reaction conditions are the same as in Figure 2. The turnover frequency is given for the rate of CO2 conversion (rCO2, dark green circles), CO conversion (rCO, purple circles) and the total conversion of CO2 and CO (rtot, black circles). Coverages are given for formate (dark green circles), CO (purple circles) and the free sites (black stars). The coverages of all other intermediates were negligible for the surfaces and reaction conditions studied here. The turnover frequency in the range 0 to 0.005 (site-1s-1) for the Cu-site is magnified as an insert in the topmost left figure.

For the Zn-site the picture is essentially reversed. Zn deactivates the surface for CO hydrogenation, as expressed by extremely low rates on the Zn-site. The CO coverage is calculated to be close to zero even without CO2 present in the feed as opposed to the Cu-site where this can be up to 0.1 ML. This has also been observed experimentally by microcalorimetric measurements that showed weaker binding of CO on ZnO-promoted Cu catalysts.[21] The hydrogenation of CO2 is significantly enhanced on the Zn-site so that the total hydrogenation rate increases with CO2 in the feed. Likewise, CO2 constitutes the major carbon source over the whole CO2 feed concentration range simulated, being largely in agreement with earlier results from Nakamura's group who established the promotional effect of Zn in CO2 hydrogenation in the context of a Cu-O-Zn ensemble as the active site.[2c, 22] A similar mechanism, where the oxygenates are adsorbed on the oxophilic promoter and hydrogen on the metal sites was also proposed for methanol synthesis on ZrO2-promoted Cu catalysts.[23]
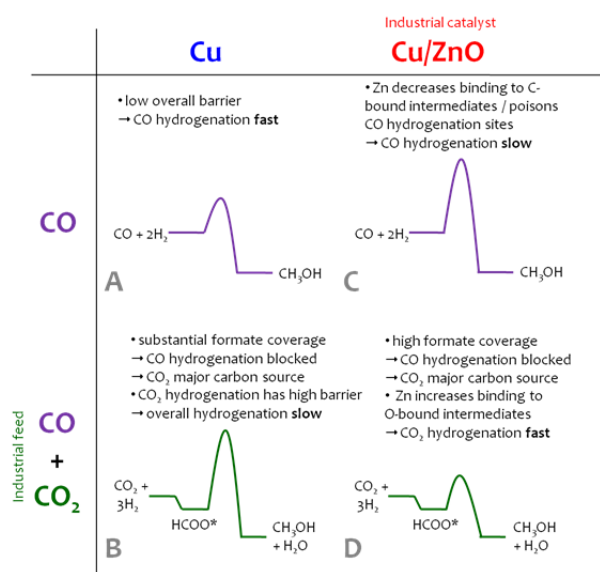

Figure 4. Schematics of the four cases (A to D) considered in this study as denoted in Figures 1-3. Case D refers to industrial conditions.

Our theoretical modeling has allowed us to define four limiting cases for Cu-based methanol synthesis catalysts and reaction conditions. These are consistent with their experimental counterparts and can comprehensively explain the experimental observations of the Cu/ZnO/Al2O3 and Cu/MgO catalysts in CO2/CO/H2 and CO/H2 feeds. The picture that emerges for methanol synthesis is summarized in Figure 4, which schematically shows the four cases A-D. Copper catalysts in the absence of ZnO can exhibit fast rates for CO hydrogenation (case A, apparent experimental activation energy Ea = 31 ± 2 kJ/mol), but deactivate with increasing formate coverage controlled by

the concentration of CO2 in the feed gas (case B, Ea = 79 ± 7 kJ/mol, cf. 77 ± 10 kJ/mol observed for polycrystalline Cu).[16] The reason for this behavior is the relatively weak interaction of oxygen atoms with pure Cu leading to a low conversion of adsorbed formate to methanol. As formate constitutes the main species on the surface, however, its conversion contributes more to the resulting methanol than the fast but rarely occurring hydrogenation of CO. Promotion of copper by ZnO, on the other hand, blocks the CO conversion sites and does hence lead to poor CO conversion rates (case C, Ea = 81 ± 2 kJ/mol). This can be rationalized by the relatively weak binding of carbon atoms by Zn. Unlike unpromoted copper Zn increases the binding of oxygen-bound intermediates and hence accelerates CO2 hydrogenation to the extent that Cu/ZnO becomes a good methanol synthesis catalyst in feeds containing CO2 (case D, Ea = 57 ± 3 kJ/mol). The important interplay of the ZnO promoter and the formate intermediate is thus that formate can only be effectively hydrogenated on Cu-based catalysts due to the Zn-modification of the Cu site, for whose CO hydrogenation activity it otherwise would be poisonous.

The choice of Cu/ZnO-based catalysts is motivated by its ability to hydrogenate CO2. As CO2 hydrogenation is less exothermic (-40.9 kJ/mol) than CO hydrogenation (-90.7 kJ/mol), CO on the other hand is beneficial in the feed gas as it shifts the thermodynamic equilibrium towards higher conversion. Under integral reaction conditions CO and water (produced by CO2 hydrogenation) are converted to CO2 (and hydrogen) via the water gas shift reaction,[2g, 24] which is fast compared to methanol synthesis on copper based catalysts and hence equilibrates.[13d, 24-25] The important role of the water gas shift reaction in industrial methanol synthesis is to enable a higher methanol formation rate at integral conditions by mitigation of product inhibition through cleaning the surface from adsorbed water. Simultaneously, new CO2 as precursor for methanol is produced. For the fundamental considerations of this work, which are based on differential conditions as the only meaningful way to investigate the reaction mechanism and especially the question of the carbon source, the secondary water gas shift reaction does not play a major role. However, we note that our theory predicts the water-gas-shift reaction to be an order of magnitude faster than CO2 hydrogenation on the active sites identified in this work for methanol synthesis.[24]

Performance catalysts will expose a distribution of different sites maximizing the beneficial thermodynamic effects of a feed mix. Thus, Figure 4 should be interpreted as representing the extreme cases of feed composition and the minimum complexity of active sites required to qualitatively explain catalytic COx hydrogenation on copper and the decisive role of the Zn promoter. Practical realizations of copper-based catalysts will exhibit a behavior that is somewhere in between these extremes and the controversial discussion of the performance of many catalysts that have been studied in the literature is explained by a superposition of the cases described Figure 4. The industrial methanol synthesis (case D) is a fixed point of reference in the parameter field that determines such superposition. By using Cu/MgO as a counter example, this study has shown that a dramatically different catalytic behavior can be achieved by changing the composition of catalyst and feed away from the industrially relevant system. The large variety of methanol synthesis activities contained for instance in Figure 2 clearly shows that comparisons of single measurements of different materials under different conditions need to be evaluated with great care. A successful research strategy needs to validate its model catalysts by also addressing a parameter variation in an attempt to approach the industrially relevant conditions.

Conclusions

The model presented here answers the questions of carbon source and of the role of ZnO. It provides a framework of functional elements to rationalize the chemical reaction system standing behind the combination of Cu and Zn active sites with a mix of CO and CO2. The catalyst mixture optimizes the reaction kinetics whereas the feed gas optimized the equilibrium thermodynamics of the system. The

present work highlights how empirical optimization found a fortunate combination of kinetics and thermodynamics. It further points to the necessity of studying the whole chemical system when further optimization is desired: changing either feed conditions or catalyst composition alone will not lead to an improved performance. With respect to desired hydrogenation of CO_2 in the context of the energy challenge[2f, 26] it can be predicted that the optimization of the catalyst composition beyond the present technical systems should be beneficial to attain better performance provided that the micro- and meso-structural features of the present system remain preserved.[27]

Experimental Section

All catalysts used in this work have been synthesized from a substitute malachite precursor, $(Cu,M)2(OH)2CO3$ (M = Zn, Mg), obtained by co-precipitation using the concept of the industrial catalyst. By this synthesis strategy, two high surface area catalysts Cu/MgO and $Cu/ZnO/Al_2O_3$ have been obtained that have experienced an analogous preparation history and exhibit a comparable microstructure with a similar Cu dispersion. This allowed a direct comparison of these performance catalysts at the same conditions regarding temperature, pressure and catalyst mass without any re-scaling in Figure 1A. Further details on the synthesis and the properties of the catalysis can be found in the SI. All catalysts tests were done in fixed bed flow reactor. The catalysts (sieve fraction 100 - 200 µm) were reduced at 523 K (1 K min−1) for at 2 hours in 20 % H_2 in He (100 mL min-1) prior to methanol synthesis at 30 bar and 503 K. Products were analysed by Gas Chromatography. The activation energies have been determined in the same reactor in the temperature range between 463 and 523 K in $CO/H_2/inert$ (14/59/27) and $CO_2/H_2/inert$ feeds (24/72/4). Details of the testing procedure can be found in the SI. For the feed gas switching experiments (Figure 1A), approximately 50 mg of catalyst have been used. After stabilization the feed gas composition was abruptly switched between a 6% CO / 8% CO_2 /59% H_2 syngas mixture and 14% CO / 59% H_2 (rest: He). For the feed gas variation measurements (Figure 2), the general feed gas composition was 14% CO_x / 59% H_2, rest He. The concentrations were gradually varied in the range 0% < CO_2 < 8% or 0% < $CO_2/(CO+CO_2)$ < 57%. After the start of the reaction, the catalysts were allowed to stabilize for 4 hours time on stream. All our measurements were performed at differential conversions to suppress the shift reaction and to avoid product inhibition. To compare activity data of our measurements to literature data, the rates have been corrected assuming a first order dependency on the hydrogen partial pressure and Arrhenius-type behaviour as described in the SI. The isotopic tracing experiments during methanol synthesis were conducted using a calibrated mass spectrometer to determine the absolute concentration of 13C-labeled methanol in the product from a syngas mix with 13C-labelled CO_2. More details can be found in the SI. The in-situ TG experiments were performed on a high pressure magnetic suspension balance by Rubotherm at 30 bar and 503 K. Prior to the experiment, the catalysts were reduced in the balance with H_2 at 523 K. Control experiments to interpret the weight changes of the catalysis are described below. Density functional theory calculations have been performed with the Quantum Espresso code[28] using a plane-wave basis set in the generalized gradient approximation with the BEEF-vdW exchange-correlation functional,[17] which explicitly takes long-range dispersion forces into account. The plane-wave cutoff used in all calculations was 500 eV and the density cutoff 5000 eV. Stepped surfaces have been modeled using a 9 layer (3x1) unit cell resulting in a slab with 3 layers in the (111) direction having monoatomic steps with a (100) geometry. In all calculations the adsorbates and the atoms in top most (111) layer are allowed to relax until forces become smaller than 0.05 eV/Å. The vibrational frequencies used to determine the zero-point energy and entropic contributions to the free energy have all been calculated within the harmonic approximation. A correction of the gas-phase errors[29] in BEEF-vdW was performed using the Quantum Espresso code as described below. For the microkinetic modeling, a mean-field microkinetic model was employed to calculate the reaction rates. The model solves the rate of methanol production under steady state conditions and treats all reaction steps as being potentially

rate limiting within the reactions paths described below. The model was solved at differential reaction conditions to match the experimental conditions, that is for low conversion to methanol (and water).

[1]   J. B. Hansen, P. E. H. Nielsen, in Handbook of Heterogenous Catalysis (Eds.: Ert, Knötzinger, Schüth, Weitkamp), Weily-VCH 2008.

[2]   a) K. C. Waugh, Catal. Lett. 2012, 142, 1153-1166; b) P. L. Hansen, J. B. Wagner, S. Helveg, J. R. Rostrup-Nielsen, B. S. Clausen, H. Topsoe, Science 2002, 295, 2053-2055; c) J. Nakamura, Y. Choi, T. Fujitani, Top. Catal. 2003, 22, 277-285; d) Y. Yang, C. A. Mims, D. H. Mei, C. H. F. Peden, C. T. Campbell, J. Catal. 2013, 298, 10-17; e) P. B. Rasmussen, P. M. Holmblad, T. Askgaard, C. V. Ovesen, P. Stoltze, J. K. Norskov, I. Chorkendorff, Catal. Lett. 1994, 26, 373-381; f) O. Martin, J. Perez-Ramirez, Catal. Sci. Technol. 2013, 3, 3343-3352; g) Y. Morikawa, K. Iwata, K. Terakura, Appl. Surf. Sci. 2001, 169–170, 11-15; h) M. Muhler, E. Törnqvist, L. Nielsen, B. Clausen, H. Topsøe, Catal. Lett. 1994, 25, 1-10; i) R. N. d'Alnoncourt, X. Xia, J. Strunk, E. Loffler, O. Hinrichsen, M. Muhler, Phys. Chem. Chem. Phys. 2006, 8, 1525-1538; j) W. Janse van Rensburg, M. Petersen, M. Datt, J.-A. van den Berg, P. van Helden, Catal. Lett. 2015, 145, 559-568.

[3]   K. Klier, V. Chatikavanij, R. G. Herman, G. W. Simmons, J. Catal. 1981, 74, 343-360.

[4]   G. C. Chinchen, P. J. Denny, D. G. Parker, M. S. Spencer, D. A. Whan, Appl. Catal. 1987, 30, 333-338.

[5]   M. Behrens, F. Studt, I. Kasatkin, S. Kühl, M. Hävecker, F. Abild-Pedersen, S. Zander, F. Girgsdies, P. Kurr, B.-L. Kniep, M. Tovar, R. W. Fischer, J. K. Nørskov, R. Schlögl, Science 2012, 336, 893-897.

[6]   a) B. Denise, R. P. A. Sneeden, Appl. Catal. 1986, 28, 235-239; b) S. Zander, E. L. Kunkes, M. E. Schuster, J. Schumann, G. Weinberg, D. Teschner, N. Jacobsen, R. Schlögl, M. Behrens, Angew. Chem. Int. Ed. 2013, 52, 6536-6540; c) J. A. Brown Bourzutschky, N. Homs, A. T. Bell, J. Catal. 1990, 124, 73-85.

[7]   M. S. Spencer, Top. Catal. 1999, 8, 259-266.

[8]   a) V. Schott, H. Oberhofer, A. Birkner, M. Xu, Y. Wang, M. Muhler, K. Reuter, C. Wöll, Angew. Chem. Int. Ed. 2013, 52, 11925-11929; b) N. Y. Topsoe, H. Topsoe, Top. Catal. 1999, 8, 267-270.

[9]   C. Holse, C. F. Elkjær, A. Nierhoff, J. Sehested, I. Chorkendorff, S. Helveg, J. H. Nielsen, J. Phys. Chem. C 2014, 119, 2804-2812.

[10]   a) J. D. Grunwaldt, A. M. Molenbroek, N. Y. Topsoe, H. Topsoe, B. S. Clausen, J. Catal. 2000, 194, 452-460; b) S. Kuld, C. Conradsen, P. G. Moses, I. Chorkendorff, J. Sehested, Angew. Chem. Int. Ed. 2014, 53, 5941-5945.

[11]   M. B. Fichtl, J. Schumann, I. Kasatkin, N. Jacobsen, M. Behrens, R. Schlögl, M. Muhler, O. Hinrichsen, Angew. Chem. Int. Ed. 2014, 53, 7043-7047.

[12]   A. Y. Rozovskii, Kinetika i Kataliz 1980, 21, 87.

[13]   a) S. Fujita, A. M. Satriyo, G. C. Shen, N. Takezawa, Catal. Lett. 1995, 34, 85-92; b) K. C. Waugh, Catal. Today 1992, 15, 51-75; c) J. Saussey, J. C. Lavalley, C. J. Bovet, Chem. Soc. Faraday Trans. 1982, 87, 1457; d) J. Yoshihara, C. T. Campbell, J. Catal. 1996, 161, 776-782.

[14]   M. Sahibzada, I. S. Metcalfe, D. Chadwick, J. Catal. 1998, 174, 111-118.

[15]   T. Fujitani, I. Nakamura, T. Uchijima, J. Nakamura, Surf. Sci. 1997, 383, 285-298.

[16]   J. Yoshihara, S. C. Parker, A. Schafer, C. Campbell, Catal. Lett. 1995, 31, 313-324.

[17]   J. Wellendorff, K. T. Lundgaard, A. Møgelhøj, V. Petzold, D. D. Landis, J. K. Nørskov, T. Bligaard, K. W. Jacobsen, Phys. Rev. B 2012, 85, 235149.

[18]   F. Studt, F. Abild-Pedersen, J. B. Varley, J. K. Nørskov, Catal. Lett. 2013, 143, 71-73.

[19]   L. C. Grabow, M. Mavrikakis, ACS Catal. 2011, 1, 365-384.

[20]   A. J. Medford, J. Wellendorff, A. Vojvodic, F. Studt, F. Abild-Pedersen, K. W. Jacobsen, T. Bligaard, J. K. Nørskov, Science 2014, 345, 197-200.

[21]   R. Naumann d'Alnoncourt, M. Kurtz, H. Wilmer, E. Löffler, V. Hagen, J. Shen, M. Muhler, J. Catal. 2003, 220, 249-253.

[22]   I. Nakamura, H. Nakano, T. Fujitani, T. Uchijima, J. Nakamura, Surf. Sci. 1998, 402–404, 92-95.

[23]   I. A. Fisher, H. C. Woo, A. T. Bell, Catal. Lett. 1997, 44, 11-17.

[24]   F. Studt, M. Behrens, F. Abild-Pedersen, Catal. Lett. 2014, 144, 1973-1977.

[25]   a) K. M. Vanden Bussche, G. F. Froment, J. Catal. 1996, 161, 1-10; b) L. Sunggyu, in Handbook of Alternative Fuel Technologies, CRC Press, 2007, pp. 297-321.

[26]   a) F. Studt, I. Sharafutdinov, F. Abild-Pedersen, C. F. Elkjær, J. S. Hummelshøj, S. Dahl, I. Chorkendorff, J. K. Nørskov, Nat. Chem. 2014, 6, 320-324; b) G. Prieto, J. Zečević, H. Friedrich, K. P. de Jong, P. E. de Jongh, Nat. Mater. 2013, 12, 34-39; c) J. Graciani, K. Mudiyanselage, F. Xu, A. E. Baber, J. Evans, S. D. Senanayake, D. J. Stacchiola, P. Liu, J. Hrbek, J. F. Sanz, J. A. Rodriguez, Science 2014, 345, 546-550.

[27]   E. L. Kunkes, F. Studt, F. Abild-Pedersen, R. Schlögl, M. Behrens, J. Catal. 2015, http://dx.doi.org/10.1016/j.jcat.2014.12.016.

[28]   G. Paolo, B. Stefano, B. Nicola, C. Matteo, C. Roberto, C. Carlo, C. Davide, L. C. Guido, C. Matteo, D. Ismaila, C. Andrea Dal, G. Stefano de, F. Stefano, F. Guido, G. Ralph, G. Uwe, G. Christos, K. Anton, L. Michele, M.-S. Layla, M. Nicola, M. Francesco, M. Riccardo, P. Stefano, P. Alfredo, P. Lorenzo, S. Carlo, S. Sandro, S. Gabriele, P. S. Ari, S. Alexander, U. Paolo, M. W. Renata, J. Phys.: Condensed Matter 2009, 21, 395502.

[29]   A. A. Peterson, F. Abild-Pedersen, F. Studt, J. Rossmeisl, J. K. Nørskov, Energy Environ. Sci. 2010, 3, 1311-1315.

.